Effect of initial plant density on modeling accuracy of the revised sparse Gash model: a case study of *Pinus tabuliformis* plantations in northern China

Yiran Li, Xiaohua Liu, Chuanjie Zhang, Zedong Li, Ye Zhao and Yong Niu

ABSTRACT

An accurate quantitative description of interception is necessary to understand regional water circulation. The revised sparse Gash model (*RSGM*) is currently used to estimate interception loss. Previous studies have proven that changes in initial plant density, which are caused by thinning, affect the accuracy of *RSGM*; however, the direct effect of initial density on modeling accuracy remains poorly understood because few studies have collected field data of the same species with various initial densities under similar site conditions. Therefore, six *Pinus tabuliformis* Carr. plantations with various initial densities were assessed from May to October 2016 in northern China. In summary, *RSGM* performs better with higher initial densities, and it cannot be suitably applied for plantations with lower initial densities, with the relative error ranging from 18.38 to 53.03%. Sensitivity analysis indicated that the predicted interception is highest sensitive to canopy structure, irrespective of initial density. The influence of climate parameters on simulated results decreased, as initial density increased. These support the notion that amending the representation of the canopy structure in the model and improving the estimation methods for determining the evaporation rate in open canopies can improve accuracy, and that the use of *RSGM* must first involve the consideration of initial density.

Key words | initial plant density, interception loss, revised sparse Gash model, sensitivity analysis, simulation accuracy

HIGHLIGHTS

- Application of the revised sparse Gash model (RSGM) in six Chinese pine plantations of different initial densities.
- RSGM still does not perform well at the sparse initial densities.
- Changes in initial plant density can affect the simulation accuracy of RSGM.
- Discuss the possibility of perfecting RSGM to improve its accuracy.
- Explore the changes in sensitivity of the parameters in RSGM under different initial densities.

Yiran Li†
Zedong Li
Yong Niu (corresponding author)
College of Forestry,
Shandong Agricultural University,
Shandong 271018,
China
E-mail: *niuyong1988@126.com*

Yiran Li†
Xiaohua Liu†
School of Soil and Water Conservation,
Beijing Forestry University,
Beijing 100083,
China

Ye Zhao
College of Biological Sciences and Technology,
National Engineering Laboratory for Tree Breeding,
Beijing Forestry University,
Beijing 100083,
China

Chuanjie Zhang†
College of Water Conservancy and Civil Engineering,
Shandong Agricultural University,
Shandong 271018,
China

†Y. R. Li, X. H. Liu and C. J. Zhang should be considered co-first authors

doi: 10.2166/nh.2020.007

GRAPHICAL ABSTRACT

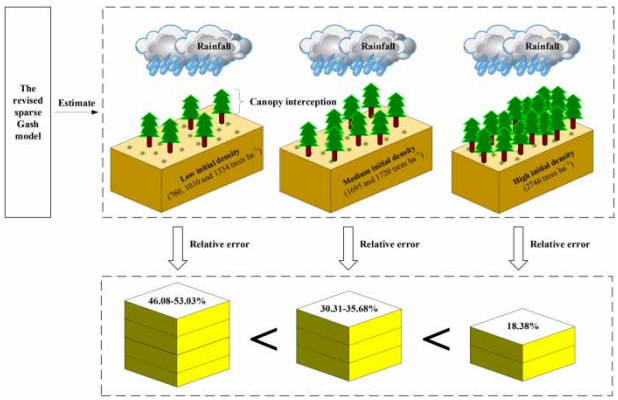

INTRODUCTION

The development of plantations has continued to increase in recent years in China (Gao *et al.* 2014; Ma *et al.* 2018), with the area under plantation increasing to 693,338 km^2 (National Forestry and Grassland Administration 2013). Nevertheless, several underlying issues, such as poor quality of plantations, have emerged because of the rapid increase in green areas. With abundant forests in northern China, water resources are considered a crucial restrictive factor for plantation growth. In these areas with limited water resources, a good understanding of ecohydrological processes plays a critical role in the essential components of water resources management and stand structure optimization.

A substantial amount of precipitation can be intercepted by and can subsequently evaporate from forest canopies (van Dijk & Bruijnzeel 2001a; Hassan *et al.* 2017). This intercepted precipitation plays a crucial role in both regional water balance in forested areas and spatial rainfall distribution (Zeng *et al.* 2000; Llorens & Domingo 2007); in addition, it contributes to the growth of woods. Models of interception loss (I), such as the original Gash model (Gash 1979), are important tools for researching ecohydrological characteristics; these models have garnered substantial attention from scholars, and several modified or improved models have now been developed, such as the sparse Gash model (Gash *et al.* 1995), the revised sparse Gash model (*RSGM*) (Valente *et al.* 1997; Limousin *et al.* 2008), and the so-called RS-Gash model (Cui & Jia 2014). Prior studies have mainly focused on the applicability of either the original Gash model or its revised versions in plantations, natural forests, or shrub forests (Sadeghi *et al.* 2015; Fernandes *et al.* 2017; Ghimire *et al.* 2017; Fathizadeh *et al.* 2018). Similarly, some previous studies have evaluated the effect of rainfall characteristics or model parameters on the prediction accuracy of the model using only a single-tree species in a particular area (Sadeghi *et al.* 2015; Su *et al.* 2016). In addition, despite some research on the response of model accuracy to tree density, available information is limited.

Tree densities, tree species, and canopy spatial arrangements are significant in improving the prediction of interception loss (Owens *et al.* 2006; Bui *et al.* 2011; Chen *et al.* 2013). Managing initial density could be more effective than altering species composition in decreasing the impacts on water resources (Licata *et al.* 2011). Furthermore, in comparison with changing forest structure variables, it could be simpler and cruder in influencing the moisture cycle of forest watersheds. Therefore, studies on hydrological modeling that have focused on initial density are considered more significant, particularly for poor-quality plantations, because of unsuitable initial density or water resources acting as restraining factors. Additionally, some studies have

investigated the relationship between initial density changes caused by thinning and the accuracy of canopy interception models. Limousin *et al.* (2008) reported that *RSGM* provides good estimates for the canopy interception of stands with different initial densities caused by thinning. Shinohara *et al.* (2015) compared the performance of three canopy interception models (Mulder, sparse Gash, and WiMo) in forests both pre- and post-thinning and concluded that the canopy interception model might be unsuitable for Japanese cedar (*Cryptomeria japonica*) forests after intensive thinning. Ma *et al.* (2020) explored the differences between the application of the sparse Gash model and the WiMo model in pre- and post-thinning plantations, respectively, and demonstrated that both models had better performance in the un-thinned stands than in the post-thinned stands. However, these observations only focused on the effects of thinning-related initial density changes on canopy interception prediction, and studies regarding the direct impact of initial plant density variations on the modeling accuracy of *RSGM* have rarely been reported. We expected a novel finding when using *RSGM* in plantations with different initial plant densities.

Initial density is the most common index of forest management in China. Since the beginning of the last century, China has afforested large swathes of land to compensate for the insufficient green area. Although the area under afforestation is rapidly increasing, the initial plant density of the same tree species in the same area is different. Moreover, as several familiar forest management measures to improve forest quality, such as thinning and replanting, are infrequently used in most regions of China, these together result in complications such as poor plantation quality. Therefore, numerous studies focusing on ecohydrological and biogeochemical fluxes as well as on either growth characteristics or economic benefits of stands with different initial densities have provided a scientific basis for further forest management in China. Furthermore, the accuracy with which the model of interception loss estimates canopy interception is considered a significant part of such forest management, particularly for the response of model simulation efficiency to initial plant density, which is a gap that cannot be ignored for the development of interception models as well as for the fine refinement management of forests. Therefore, the objectives of the present study were to explore the effect of initial plant densities on the predicted accuracy of *RSGM* and to evaluate the impact of different initial densities on model parameters as well as examine the possibility of perfecting the model to improve its accuracy.

MATERIALS AND METHODS

Site description and experimental design

The research site (Figure 1) is located 8 km northeast of Mount Tai (Northern China) in the Yaoxiang National Forest Park (E11°05′39″–117°09′26″, N36°17′58″–36°20′30″). The research site elevation ranges from 400 to 956 m (average: 710 m). This region is located in the warm temperate zone and has a semi-humid and monsoon climate, with a mean annual temperature of 18.5 °C and a mean annual frost-free period of 198 days. The multi-year average precipitation is 727.9 mm, with 75% of the annual precipitation being concentrated from June to September. The soil type is brown soil. The underlying rock is ancient gneiss of a high metamorphic grade, with a thickness ranging from 10 to 90 cm; in most areas, thickness ranges from 30 to 50 cm. Vegetation types belong to coniferous and deciduous broad-leaved forests in the warm temperate zone, and the main tree species include *Pinus tabuliformis*, *Quercus acutissima* Carr., *Pinus densiflora* Sieb., *Robinia pseudoacacia*, and *Castanea mollissima* (Sun *et al.* 2019).

In the study area, six plots (each with a projection area of 100 m^2, length of 20 m, and width of 5 m) were set up according to the initial densities of *P. tabuliformis* plantation as follows: (1) 720 trees ha^{-1}; (2) 1,010 trees ha^{-1}; (3) 1,334 trees ha^{-1}; (4) 1,695 trees ha^{-1}; (5) 1,720 trees ha^{-1}; and (6) 2,746 trees ha^{-1}. We conducted a forestland survey in March 2016 (Table 1) and installed the *HOBO* automatic weather station (*Onset*, *USA*) surrounding the open area of the sample plots to collect necessary meteorological data such as rainfall, wind speed, and radiation. The weather station collected data at 15-min intervals, and we downloaded the data once a month. Because the six plots are relatively close in terms of distance and there is little change in meteorological factors, only one meteorological station was installed.

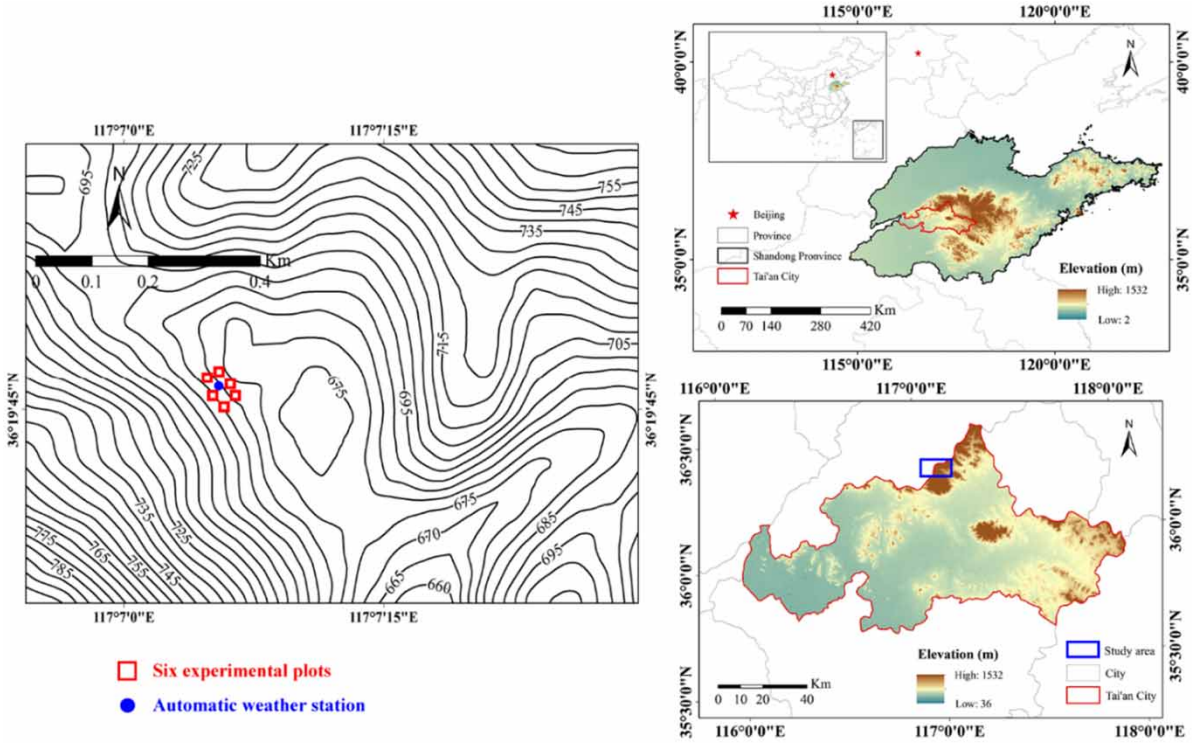

Figure 1 | Study plot location.

Table 1 | Investigation results of stand plots

Plot	*Sp.*	*Sl.* (°)	*Id* (trees ha^{-1})	*TDP* (trees)	*Ah* (m)	*ADBH* (cm)	*c*
1	*P. tabuliformis*	22	760	8	10.12 ± 0.41	17.87 ± 0.79	0.74
2		23	1,010	12	8.98 ± 0.48	16.88 ± 1.03	0.75
3		21	1,334	14	7.44 ± 0.46	15.04 ± 0.72	0.78
4		23	1,695	16	9.04 ± 0.52	13.98 ± 0.81	0.80
5		25	1,720	17	7.01 ± 0.34	12.25 ± 0.75	0.80
6		22	2,746	28	12.18 ± 0.63	15.19 ± 0.58	0.70

ADBH, average diameter at breast height (mm); *Sp.*, species; *Sl.*, slope (°); *Id*, initial density (trees ha^{-1}); *TDP*, tree density per plot (trees); *Ah*, average height (m); *c*, canopy cover.

Field measurements

Total precipitation (*TP*) was determined according to the data from the automatic weather station. Due to the proximity of the measured sample plots to each other, only one station was placed in the central position relative to each plot.

Three PVC tubes (*DN90*) with a length of 8 m and an inner diameter of 9 cm were cut open to collect throughfall (*TF*) in each plot. To avoid the influence of herbs on *TF* collection, the collectors were arranged parallel to the slope along with the sample sites and the height from the collector to the ground was ≥50 cm, connecting the collecting barrel at the bottom of the pipe (Sheng *et al.* 2014; Ji & Cai 2015). We measured the amount of water in the collecting barrel after each rainfall event. *TF* depth (mm) was calculated using the following equation:

$$TF = \frac{3 \times V \times 1000}{3 \times L \times W \times \cos\alpha} \quad (1)$$

where V is the amount of water collected in the collecting barrel after each rainfall event (L), L is the length of the PVC tube (m), W is the inner diameter of the PVC tube (m), α is the slope of the sample plots (°), and $L \times W \times cos\,\alpha$ is the cross-sectional area of the PVC tube (m^2).

Based on the survey results of the sample plots, the trees were categorized into three classes based on diameter at breast height, and three trees from each class were selected as samples. To measure stemflow (*SF*), a rubber pipe cut in the middle was stapled onto the trunks in a spiral shape. The gap between the rubber pipe and trunk was sealed with silicone, the bottom of the rubber pipe was connected to a collecting bucket, and the amount of water collected in this bucket was measured after each rainfall event. *SF* depth (mm) was calculated using the following equation:

$$SF_j = \frac{1}{M}\sum\nolimits_{i=1}^{n} \frac{G_n}{K_n} M_n \tag{2}$$

where M is the mean number of trunk plants in the projected area of the plot, n is the number of the diameter class, G_n is the amount of *SF* in each diameter class (mm), K_n is the projected canopy area in each diameter class (cm^2), and M_n is the number of trees in each diameter class.

REVISED SPARSE GASH MODEL

Formula

The original Gash model was proposed by Gash (1979). For simplicity, some assumptions have been made: (1) a series of discrete storms are used to represent the real rainfall pattern, and there is a sufficiently long interval between these storms to allow the canopy and trunks to dry; (2) the conditions of rainfall and evaporation remain sufficiently similar throughout all storms during this period; and (3) there is no water drip from the canopy during wetting-up, and large amount of water on the canopy rapidly evaporates at the end of a storm. The original Gash model was also revised based on these assumptions (Gash *et al.* 1995; Valente *et al.* 1997; Limousin *et al.* 2008). In the present study, the following equation of *RSGM* was used, which is used for calculating canopy interception that was proposed by Valente *et al.* (1997) and simplified by Limousin *et al.* (2008):

$$\sum_{j=1}^{n+m} I_j = c\sum_{j=1}^{m} P_{G,j} + \sum_{j=1}^{n} \frac{c\bar{E}}{\bar{R}}(P_{G,j} - P'_G) + c\sum_{j=1}^{n} P'_G + qcS_{tc} + cp_{tc}\sum_{j=1}^{n-q}\left(1 - \frac{\bar{E}}{\bar{R}}\right)(P_{G,j} - P'_G) \tag{3}$$

where n is the number of rainfall events during which the canopy reached saturation, m is the number of rainfall events that were insufficiently large to saturate the canopy, c is the fraction of canopy cover, P_G is the total rainfall amount (mm), $\bar{E}$ is the wet canopy evaporation rate per unit area of canopy cover (mm; calculated by the Penman–Monteith equation) (Gash *et al.* 1995; Valente *et al.* 1997; Limousin *et al.* 2008), $\bar{R}$ is the mean rainfall intensity (mm/h), P'_G is the minimum amount of precipitation required to saturate the canopy (mm), $p_{tc} = p_t/c$ is the proportion of rain diverted into *SF* per unit area of cover, $S_{tc} = S_t/c$ is the stem storage capacity per unit cover area, and q is the number of saturated trunks.

Derivation of the parameters used in the model

It was evident that the canopy storage capacity (S) is an important parameter in the model; in the present study, S was estimated using the original regression method based on the relationship between *TP* and *TF*. This method was proposed by Leyton *et al.* (1967); owing to its effectiveness because of its simplicity (Liu 1998), this method has been used more often than the method described by Klaassen *et al.* (1998) as well as has been used by Gash & Morton (1978) and Gash (1979). André *et al.* (2008) reported that the estimated performance of Leyton's approach is better than a spraying laboratory experiment and mechanistic modeling exercise.

The minimum amount of water required to saturate the canopy was determined using the equation provided by Limousin *et al.* (2008):

$$P'_G = -(\bar{R}/\bar{E})S_c \ln(1 - (\bar{E}/\bar{R})) \tag{4}$$

where $S_c = S/c$ is the canopy storage capacity per unit area of cover (in mm).

The minimum amount of water that can fill the trunk storage capacity is calculated using the following equation and is denoted as P'_G (Valente *et al.* 1997; Limousin *et al.* 2008):

$$P'_G = (\bar{R}/(\bar{R} - \bar{E}))(S_{tc}/p_{tc}) + P'_G \quad (5)$$

In addition, *TF* and *SF* can be simulated using the following equations provided by the model:

$$\sum_{j=1}^{q} SF_j = cp_{tc} \sum_{j=1}^{q} (1 - (\bar{E}/\bar{R}))(P_{G,j} - P'_{G,j}) - qcS_{tc} \quad (6)$$

$$\sum_{j=1}^{n+m} TF_j = \sum_{j=1}^{n+m} P_{G,j} - \sum_{j=1}^{n+m} I_j - \sum_{j=1}^{q} SF_j \quad (7)$$

Sensitivity analysis

In the present study, we referred to separate sensitivity analyses in previous studies for each density (cf. Valente *et al.* 1997; Fan *et al.* 2014; Fathizadeh *et al.* 2018; Liu *et al.* 2018), and S, c, $\bar{E}$, $\bar{R}$, S_t, and p_t were tested in the range of an increase and decrease by up to 50% of their original values and in terms of the results of models compared with field values.

RESULTS

Rainfall partitioning

In the present study, 8 h was considered the standard for dividing rainfall events. Based on rainfall data from May 2016 to October 2016, a total of 28 rainfall events with a total amount of 430.3 mm and a mean of 15.4 mm were recorded in the study area. Based on individual rainfall events, the maximum amount, duration, and intensity of rainfall in the plots were 73.7 mm, 37 h, and 26.32 mm/h, respectively, and the corresponding minimum values were 1.1 mm, 0.75 h, and 0.08 mm/h, respectively.

The rainfall distribution components of *P. tabuliformis* plantation of different densities varied during the study period (Table 2). With the same total rainfall, *TF* decreased and *I* increased with increasing initial density, but they increased and decreased when the initial density increased from 1,720 to 2,746 trees ha^{-1}, respectively. Typically, *TF* and *I* tended to increase with increasing initial density during the study period. By contrast, *SF* initially increased with increasing initial density, following which it decreased when initial density increased from 1,334 to 1,720 trees ha^{-1} and increased further when initial density increased from 1,720 to 2,746 trees ha^{-1}. In general, *SF* decreased with increasing density.

Model parameters

We calculated the parameters of *RSGM* using the previously described methods (Table 3). S, estimated from the regression between *TF* and *TP* (Figure 2), increased with increasing initial density. The value of S for 2,746 trees ha^{-1} (3.973 mm) was approximately four times greater than that for 720 trees ha^{-1} (0.894 mm). Values generated for S_c and P'_G ranged from 1.207 mm (for 720 trees ha^{-1}) to 5.706 mm (for 2,746 trees ha^{-1}) and from 1.229 mm (for 720 trees ha^{-1}) to 5.807 mm (for 2,746 trees ha^{-1}), respectively. Furthermore, the variation trends of S_c and P'_G were the same as that of S, and the first two parameters for 2,746 trees ha^{-1} were approximately five times greater than those for 720 trees ha^{-1}. Similar findings were obtained for S_t, p_t, and P'_G (S_t and p_t were estimated from the regression between *SF* and *TP*, as shown in Figure 3); they typically increased with increasing initial density, and their values

Table 2 | Rainfall redistribution composition of *P. tabuliformis* forests

Plot	*Sd.* (trees ha^{-1})	*TP* (mm)	*TF* (mm)	*SF* (mm)	*I* (mm)
1	720	430.3	357.9	1.6	70.8
2	1,010		316.5	20.3	93.6
3	1,334		296.8	23.6	109.9
4	1,695		286.2	19.7	124.4
5	1,720		277.2	22.2	131.0
6	2,746		280.1	25.3	124.9

TP, total precipitation (mm); *TF*, throughfall (mm); *SF*, stemflow (mm); *I*, interception loss (mm).

Table 3 | Parameters of *RSGM* for *P. tabuliformis* plantation

Plot	*Id* (trees ha^{-1})	*S* (mm)	S_c (mm)	S_t (mm)	p_t	*c*	P'_G (mm)	P''_G (mm)
1	720	0.894	1.207	0.035	0.006	0.74	1.229	7.244
2	1,010	1.281	1.708	0.394	0.073	0.75	1.738	7.394
3	1,334	2.361	3.027	0.404	0.081	0.78	3.027	8.234
4	1,695	2.774	3.467	0.414	0.073	0.80	3.529	9.422
5	1,720	3.076	3.797	0.363	0.075	0.81	3.865	8.865
6	2,746	3.937	5.706	0.545	0.094	0.69	5.807	11.795

Id, initial density (trees ha^{-1}).

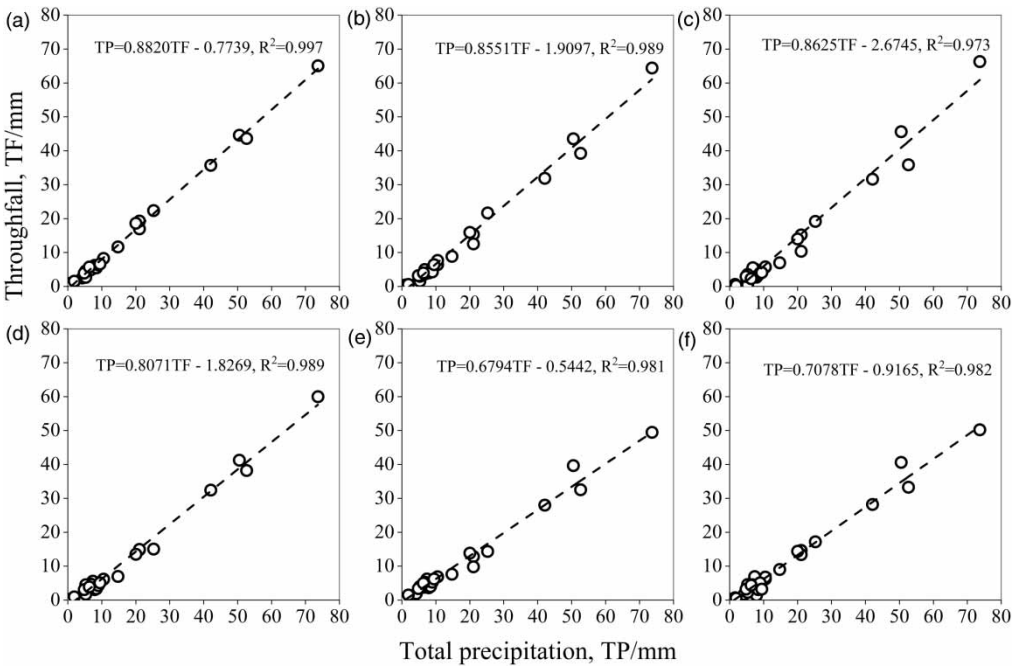

Figure 2 | Relationship between *TF* and *TP* for rainfall events. In the upper left of each figure, lowercase letters represent the sample plots with different initial densities (a = 720 trees ha^{-1}, b = 1,010 trees ha^{-1}, c = 1,334 trees ha^{-1}, d = 1,695 trees ha^{-1}, e = 1,720 trees ha^{-1}, and f = 2,746 trees ha^{-1}); the same is true in Figure 5. Each circle denotes a rainstorm event.

ranged from 0.035 mm (for 720 trees ha^{-1}) to 0.545 mm (for 2,746 trees ha^{-1}) for S_t, from 0.006 (for 720 trees ha^{-1}) to 0.096 (for 2,746 trees ha^{-1}) for p_t, and from 7.244 mm (for 720 trees ha^{-1}) to 11.795 mm (for 2,746 trees ha^{-1}) for P''_G.

Estimated results

The simulated *TF* value was overestimated, whereas the simulated *I* and *SF* values were less than the measured values (Table 4). The simulated *I* and *SF* values showed a uniform variation trend during the study period, with calculations ranging from 36.0 mm (for 720 trees ha^{-1}) to 104.4 mm (for 2,746 trees ha^{-1}) and from 1.6 mm (for 720 trees ha^{-1}) to 19.6 mm (for 2,746 trees ha^{-1}), respectively. Moreover, the simulated *TF* value decreased with an increasing initial density as a whole, differing from the trend of measured values, and ranged from 306.3 mm (for 2,746 trees ha^{-1}) to 392.7 mm (for 720 trees ha^{-1}). In addition, the simulation results indicated that irrespective of the initial density, there was substantially high *I* resulting from evaporation from saturation until rainfall stopped (6.75–28.33%) and after rainfall stopped (62.00–67.85%), and the

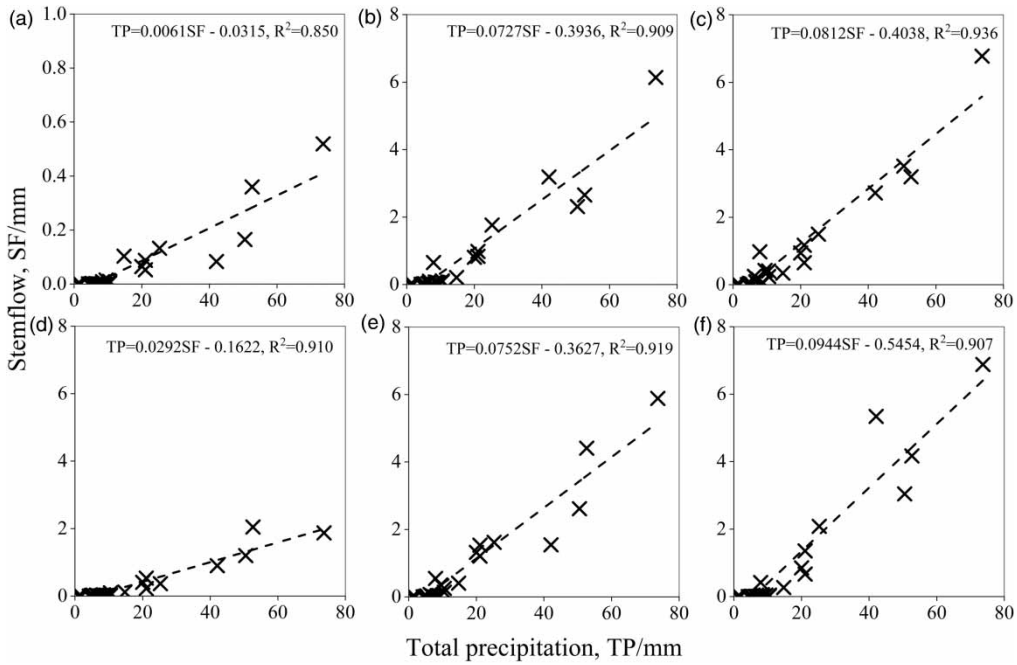

Figure 3 | Relationship between *SF* and *TP* for rainfall events. Each circle denotes a rainstorm event. In the upper left corner of each figure, lowercase letters represent sample plots with different initial densities (specific densities are the same as those in Figure 2).

Table 4 | Simulation results of *RSGM*

	Id **(trees ha^{-1})**					
Components of the model	**720**	**1,010**	**1,334**	**1,695**	**1,720**	**2,746**
For m small storms, insufficient to saturate the canopy (mm)	2.34	3.55	5.17	5.31	5.37	18.09
Wetting-up the canopy, for n storms > P'_G that saturate the canopy (mm)	0.40	0.55	0.88	1.41	1.26	1.26
Evaporation from saturation until rainfall ceases (mm)	10.21	10.02	9.58	9.53	9.44	7.05
Evaporation after rainfall stops (mm)	22.34	30.74	49.58	63.79	70.74	70.86
Evaporation from trunks (mm)	0.75	8.22	7.77	7.31	6.49	7.18
Simulated interception loss (mm)	36.0	53.1	73.0	87.1	93.3	104.4
Simulated *TF* (mm)	392.7	358.6	337.5	326.5	319.2	306.3
Simulated *SF* (mm)	1.6	18.7	19.9	16.8	17.8	19.6

lowest *I* occurred under saturated canopy conditions (1.10–1.35%). With the exception of the amount of evaporation from canopy saturation until rainfall stopped and from trunks, the other model components increased with increasing initial density.

We used the mean of the absolute error and relative error to describe the simulation accuracy of *RSGM* for *I*, *TF*, and *SF* (Figure 4). Regarding *SF*, an increase in initial density decreased the absolute error; in general, there was a tendency toward the lower absolute error of predicted *TF* and *SF* with increasing initial density, whereas the opposite was observed for *I*. Although there was a corresponding slight upward and downward trend in the absolute errors of *TF* and *I* when the initial density varied from 720 to 1,750 trees ha^{-1}, the above-mentioned conclusion was obtained irrespective of this trend. These relationships are presented in Figure 4(a).

Similarly, as shown in Figure 4(b), for *I*, there was a clear negative correlation between initial density and relative error, which ranged from 18.38% (for 2,746 trees ha^{-1}) to 53.03% (for 720 trees ha^{-1}). However, for *SF*, there was a general positive correlation between initial density and relative error, which ranged from 2.01% (in 720 trees ha^{-1}) to 21.55% (in 2,746 trees ha^{-1}). Regarding *TF*, although the trend of relative error with initial density was as variable as the trend of absolute error, the difference was that the variation of the former was more similar to the convex type.

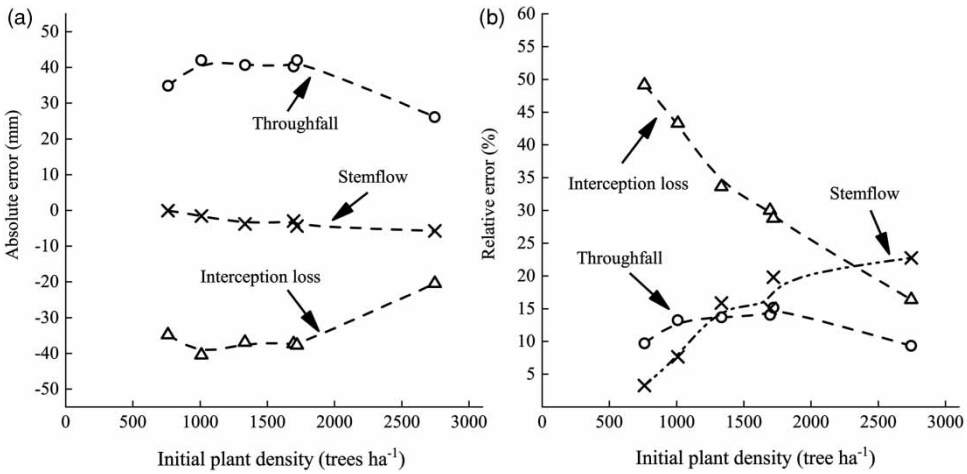

Figure 4 | The error between the simulated and measured values of interception varied with the initial density, including (a) absolute error and (b) relative error.

The relative error of *TF* in high-density stands was only slightly smaller than that in low-density stands (10.14 and 10.50%, respectively), and the highest relative error was noted in medium-density stands (15.85% in 1,720 trees ha^{-1}).

Sensitivity analysis

Figure 5 illustrates the sensitivity analysis results for the variation of predicted *I*. Besides $\bar{R}$, all remaining parameters – *S*, *c*, $\bar{E}$, S_t, and p_t – showed a positive correlation with the predicted *I*. Moreover, with a 50% increase or decrease in all the parameters tested, the representation indicates that *S* was the chief parameter for the change in predictions regardless of the initial density, which can result in a maximum change of ±30% in calculation, and the minimum influence on the prediction of interception was provided by p_t. Subsequently, the effect of $\bar{E}$ on the prediction results tended to be higher than that of $\bar{R}$ when the parameters

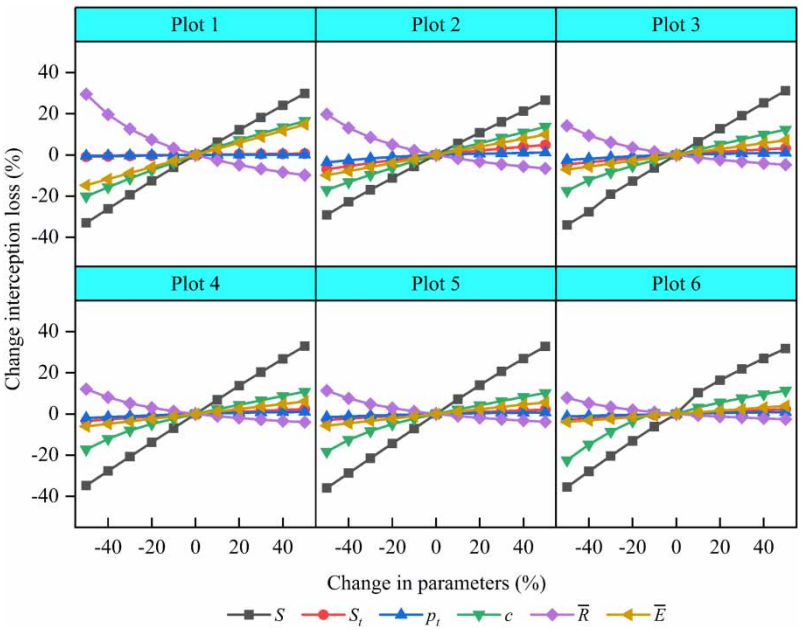

Figure 5 | Sensitivity analysis of *RSGM* for change in predicted *I*. *S*, canopy storage capacity; $\bar{R}$, mean rainfall intensity; *c*, canopy cover; $\bar{E}$, wet canopy evaporation rate per unit area of canopy cover; S_t, stem storage capacity; and p_t, drainage partitioning coefficient. The lowercase letters on the right side of the longitudinal axis represent the samples of different initial densities in each figure, and the exact meaning is the same as in Figure 2.

changed in the range of 0 to +50%. However, when the parameters tested changed from −50 to 0%, the influence of $\bar{R}$ was higher than that of $\bar{E}$ for all plots. Furthermore, higher initial density corresponded to lower influence of $\bar{R}$ and $\bar{E}$. With a 50% decrease in $\bar{R}$ and c, the influence of $\bar{R}$ on the prediction results was higher than that of c, and there was a change in the corresponding average simulated cumulative I of 29.38 and 20.12% within 760 trees ha^{-1}, and 19.69 and 17.01% within 1,010 trees ha^{-1}. Further, the effect of c on simulation was higher than that of $\bar{R}$ when the initial density exceeded 1,010 trees ha^{-1}.

DISCUSSION

During the study period, the average I measured in *P. tabuliformis* plantation plots ranged from 16.46 to 30.44% of the total rainfall. Typically, I in temperate coniferous forests ranges from 10 to 60% (Teklehaimanot *et al.* 1991; Loustau *et al.* 1992; Licata *et al.* 2011), with I measured in our study falling in the upper half of this range. The I range in our study is consistent with those for the main plantation forest in China (14.7–31.8%) and coniferous forests (21.0–48.0%; Carlyle-Moses 2004; Wei *et al.* 2005), and it is within the range of the interception of *P. tabuliformis* in various study areas in China (15.7–36.9%; Fang *et al.* 2013). Valente *et al.* (1997) obtained similar results there was a lower interception in less dense forests. Results of the measurement of rainfall partitioning at different initial densities indicated that more rainfall penetrated the canopy and entered the next layer, thereby affecting the hydrology of the forest ecosystem and contributing to plant growth, and appropriate thinning may improve the rainwater use efficiency of forests.

In the present study, the estimated S ranged from 0.894 to 3.937 mm and was lower in low-density stands than in high-density stands. According to Deguchi *et al.* (2006), the estimated S in different regions worldwide ranges from 0.25 to 1.69 mm, and this range is lower in medium-density (1,334, 1,695, and 1,720 trees ha^{-1}) and high-density stands (2,746 trees ha^{-1}). The reason for this might be that *P. tabuliformis* plantation in this study was an artificial coniferous pure forest with a vegetation type that is different from that in the above-mentioned literature (such as secondary broad-leaved deciduous forest, mature mixed deciduous forest, hardwood forest, and mixed White Oak forest). Therefore, we compared our estimated S with the variation range (0.1–3.0 mm) of S in coniferous forests under different initial densities, as summarized by Llorens & Gallart (2000). We found that the S value in *P. tabuliformis* forests remained higher than that in coniferous forests of similar density such as *Pinus sylvestris*, *Picea sitchensis*, and *Pinus elliottii*. This may be due to the distinctive broad-ovate crown profile of *P. tabuliformis*. The developed sclerenchyma on the epidermis of needles and sunken pores can provide appropriate conditions for *P. tabuliformis* to carry more water than the coniferous forests evaluated in other studies (China Agricultural Encyclopedia Forestry Volume Editorial Committee 1989). Remarkably, the variation trend of the S value of these species exhibited an approximate wavy line with an increasing initial density, rather than following a linear trend as observed in the present study. We propose that the S value of the same coniferous species exhibits certain threshold values with increasing initial density and that the S value will continue to increase and decrease. Differences in results between this and other studies may be due to the fact that the maximum initial density of the *P. tabuliformis* plantation in this study (2,746 trees ha^{-1}) was lower than the initial density corresponding to the theoretical first threshold of S of *P. tabuliformis* artificial forests. Similarly, we hypothesize that if the initial density continues to increase, the S value of *P. tabuliformis* artificial forests will show the same trend with increasing initial density as previously reported.

In our study, fixed growing season parameters were used in *RSGM* to predict total interception, which was the same as those reported by Fan *et al.* (2014) and Junqueira Junior *et al.* (2019). Indeed, the rigor of the derivation process may be inadequate; however, it is possible to use fixed parameters to obtain satisfactory estimates of growing season interception (Wallace & McJannet 2008; Ghimire *et al.* 2012; Fan *et al.* 2014). Because the study was conducted during the growing season, the canopy and climatic parameters changed slightly. Moreover, the variation of the canopy and climatic parameters will compensate for each other; therefore, the error of the final simulation of interception may be considered minimal, as discussed by Wallace & McJannet (2008) and Fan *et al.* (2014). The type of variations for the final simulation results produced within a certain period when fixed parameters are used at different time scales in *RSGM* to predict annual interception remains

unclear and requires further investigation. Recently, a study used models with fixed parameters for the dormant and growing seasons (Ma *et al.* 2019), respectively. The model showed good performance for both periods; however, some parameters seemed to considerably vary between the two periods, implying that it is still questionable whether fixed canopy structures and climatic parameters can be used for simulating annual canopy interception or for a period spanning the dormant and growing seasons. Moreover, Zhang *et al.* (2018) used variable parameters to run *RSGM* to estimate canopy interception in a deciduous shrub; i.e., $\bar{R}$ and $\bar{E}$ represent the average values during all hours in each rainfall event. It remains to be demonstrated whether this approach can be used to obtain a good result in forests.

In the present study, although we used *RSGM*, it demonstrated better performance in *P. tabuliformis* forests with higher-density and could not be applied well in lower-density forests; moreover, the relative error decreased with increasing initial density and the revised model tended to overestimate *TF* and underestimate *SF* and *I*, which is similar to the findings obtained by Limousin *et al.* (2008) and Ma *et al.* (2020). Although *c* was added to the revised version of the model to further describe the characteristics of canopy structure and vegetation density along with *S* (Gash *et al.* 1995), it was not adequate. The indirect and complete estimation of the complex canopy structure is a significant channel to improve the simulation accuracy of the model. However, *c* can only interpret the horizontal structure of the canopy and cannot adequately express canopy thickness, vegetation density, and other structural and physiological parameters, which may affect simulation accuracy, particularly in forests with lower density. van Dijk & Bruijnzeel (2001a) proposed correcting the revised model by supplementing the leaf area index (*LAI*) and expounding its relationship with *S* and *c*; they considered that *LAI* was linearly related to canopy capacity rather than to canopy cover in 'constant physiognomy and configuration' and accordingly presented an application of this version (van Dijk & Bruijnzeel 2001b). Nevertheless, this version of the model is based on the hypothesis that canopy capacity is not affected by initial density, and because this hypothesis was evidently contrary to the results of the present study, it may not be a highly effective solution to improve the accuracy of the model from the root. The canopy structure must be effectively integrated into the analytical Gash model to improve model accuracy. Ginebra-Solanellas *et al.* (2020) suggested that raindrop characteristics and leaf biomechanical properties may influence the modeling of the dynamic processes of forest canopy interception. Furthermore, reconstructing the method of estimating *S* may be the correct direction to reduce model simulation errors. Valente *et al.* (2020) proposed a new procedure to estimate *S* by inverse extrapolation. This method has been validated at the single-tree scale but has not been widely used yet because it may not be effective for regions without historical monitoring information.

Differences in initial plant density may affect forest hydrological processes and the nutrient cycle, subsequently influencing vegetation growth. This will be accompanied by differences in forest structure variables. Therefore, we also considered the implication of the effects of changes in forest structure variables on the modeling accuracy of the revised Gash model, although it is not detailed enough. Moreover, Fathizadeh *et al.* (2017) showed that *S* and *I* have strong relationships with wood area index, except *LAI* and *c*, and supported the idea that the studies for canopy structure variables can considerably enhance the performance of the hydrological models. Indeed, we plan to continue the work of Fathizadeh *et al.* (2017) to conduct future detailed studies on this subject; however, for now, this study only discussed the influence of initial plant density on the modeling accuracy of the revised Gash model owing to the limitation of observation equipment and measures.

Sensitivity analysis showed that *S* demonstrated absolute dominance in medium- and higher-density forests, which was similar to the results reported by Dykes (1997), Liang (2014), and Su *et al.* (2016); however, *S*, the chief parameter for simulated results, is not dependent on the density. The influence of $\bar{R}$ and $\bar{E}$ gradually decreased as the initial density increases. This may be due to the particular characteristics of precipitation during the study period (relatively long rainfall duration, intermittent rainfall patterns, and a relatively large number of moderate and extreme rainfall events). Most rainfall occurred at night during the study period, which may be the reason for the lesser contribution of the evaporation rate in the present study compared with that in other studies (Loustau *et al.* 1992; Deguchi *et al.* 2006; Fathizadeh *et al.* 2018). Linhoss & Siegert (2016) reported that storm duration, canopy

storage, and solar radiation were extremely important for canopy interception model sensitivity. Lower-density forests exhibit larger forest gaps, larger crown width, and thinner crown thickness than higher-density forests, which may explain the reason for the climatic parameters being more sensitive at lower densities. In addition, Linhoss & Siegert (2016) have reported that the estimation of the evaporation rate using the Penman–Monteith approach appears preferable for canopies that are not completely ventilated rather than for sparse forests and the methods for estimating the evaporation rate in sparse forests should be investigated. Therefore, there have been studies that have attempted to use the wet-bulb method instead of the Penman–Monteith approach to derive the evaporation rate at the single-tree or sparse forest level when using the Gash-type models (e.g., Ma *et al.* 2019; Valente *et al.* 2020), and model performance using the former is superior to the latter. This implies that improving the methods used for estimating meteorological parameters in models could be a valid direction for sparse forests.

CONCLUSIONS

The average cumulative measured I ranged from 16.46 to 30.44% of gross rainfall in *P. tabuliformis* plantations with different initial densities, and the interception was positively associated with initial plant density. The results obtained using the revised Gash model suggested that a relatively good consistency exists between the modeled and estimated interceptions in higher-density forests and that simulation accuracy enhances with an increase in the density. This may be attributable to the revised model being inadequate with respect to certain biological characteristics of *P. tabuliformis* plantations and the expression of the canopy structure of the sparse forest, and these weaknesses are magnified during the simulation of *P. tabuliformis* plantation. The predicted interception was higher sensitive to the canopy structure, irrespective of the initial density, and the close stands were less susceptible to the effects of the climate parameters on accuracy than the sparse stands. Therefore, it is crucial to effectively optimize and modify parameters describing the canopy structure in *RSGM* for improving simulative accuracy while ensuring the simplicity of the model and identifying and developing direct observation or estimation methods that are more appropriate to describe the evaporation rate for the open canopy is an effective approach to improve the operational performance of *RSGM* in sparse forests. Moreover, it is imperative to further demonstrate the influence of estimated mean values of climatic parameters at different time scales on simulation accuracy. Most importantly, the impact of initial planting density on the simulation results cannot be ignored when using *RSGM* to quantify canopy interception. The applicability of *RSGM* in sparse forest remains to be investigated until the model can be further improved or validated in the application area.

ACKNOWLEDGEMENTS

This work was funded by the Natural Science Foundation of Shandong Province of China project (No. ZR2016DB12) and a project of the Key Laboratory of Water Saving Irrigation Project of Ministry of Agriculture (Farmland Irrigation Research Institute of Chinese Academy of Agricultural Sciences, No. FIRI2018-04).

DATA AVAILABILITY STATEMENT

Data cannot be made publicly available; readers should contact the corresponding author for details.

REFERENCES

André, F., Jonard, M. & Ponette, Q. 2008 Precipitation water storage capacity in a temperate mixed oak-beech canopy. *Hydrological Processes* **22** (20), 4130–4141. doi:10.1002/hyp.7013.

Bui, X. D., Shusuke, M. & Takashi, G. 2011 Effect of forest thinning on overland flow generation on hillslopes covered by Japanese cypress. *Ecohydrology* **4** (3), 367–378. doi:10.1002/eco.135.

Carlyle-Moses, D. E. 2004 Throughfall, stemflow, and canopy interception loss fluxes in a semi-arid Sierra Madre Oriental matorral community. *Journal of Arid Environments* **58** (2), 181–202. doi:10.1016/S0140-1963(03)00125-3.

Chen, S., Chen, C., Zou, C. B., Stebler, E., Zhang, S., Hou, L. & Wang, D. 2013 Application of Gash analytical model and parameterized Fan model to estimate canopy interception of a Chinese red pine forest. *Journal of Forest Research* **18** (4), 335–344. doi:10.1007/s10310-012-0364-z.

China Agricultural Encyclopedia Forestry Volume Editorial Committee 1989 *China Agricultural Encyclopedia Forestry, Volume (II)*. Agricultural Press, Beijing.

Cui, Y. & Jia, L. 2014 A modified Gash model for estimating rainfall interception loss of forest using remote sensing observations at regional scale. *Water* **6** (4), 993–1012. doi:10.3390/w6040993.

Deguchi, A., Hattori, S. & Park, H. 2006 The influence of seasonal changes in canopy structure on interception loss: application of the revised Gash model. *Journal of Hydrology* **318** (1–4), 80–102. doi:10.1016/j.jhydrol.2005.06.005.

Dykes, A. P. 1997 Rainfall interception from a lowland tropical rainforest in Brunei. *Journal of Hydrology* **200** (1–4), 260–279. doi:10.1016/S0022-1694(97)00023-1.

Fan, J., Oestergaard, K. T., Guyot, A. & Lockington, D. A. 2014 Measuring and modeling rainfall interception losses by a native Banksia woodland and an exotic pine plantation in subtropical coastal Australia. *Journal of Hydrology* **515**, 156–165. doi:10.1016/j.jhydrol.2014.04.066.

Fang, S., Zhao, C., Jian, S. & Yu, K. 2013 Canopy interception of *Pinus tabulaeformis* plantation on Longzhong Loess Plateau, North-west China: characteristics and simulation. *Chinese Journal of Applied Ecology* **24** (06), 1509–1516. doi:10.13287/j.1001-9332.2013.0326.

Fathizadeh, O., Hosseini, S. M., Zimmermann, A., Keim, R. F. & Darvishi Boloorani, A. 2017 Estimating linkages between forest structural variables and rainfall interception parameters in semi-arid deciduous oak forest stands. *Science of the Total Environment* **601–602**, 1824–1837. doi:10.1016/j.scitotenv.2017.05.233.

Fathizadeh, O., Hosseini, S. M., Keim, R. F. & Boloorani, A. D. 2018 A seasonal evaluation of the reformulated Gash interception model for semi-arid deciduous oak forest stands. *Forest Ecology and Management* **409**, 601–613. doi:10.1016/j.foreco.2017.11.058.

Fernandes, R. P., Silva, R. W. D. C., Salemi, L. F., Andrade, T. M. B. D., Moraes, J. M. D., Dijk, A. I. J. M. & Martinelli, L. A. 2017 The influence of sugarcane crop development on rainfall interception losses. *Journal of Hydrology* **551**, 532–539. doi:10.1016/j.jhydrol.2017.06.027.

Gao, Y., Zhu, X., Yu, G., He, N., Wang, Q. & Tian, J. 2014 Water use efficiency threshold for terrestrial ecosystem carbon sequestration in China under afforestation. *Agricultural and Forest Meteorology* **195–196**, 32–37. doi:10.1016/j.agrformet.2014.04.010.

Gash, J. H. C. 1979 An analytical model of rainfall interception by forests. *Quarterly Journal of the Royal Meteorological Society* **105**, 43–55. doi:10.1002/qj.49710544304.

Gash, J. H. C. & Morton, A. J. 1978 An application of the Rutter model to the estimation of the interception loss from Thetford Forest. *Journal of Hydrology* **38**, 49–58. doi:10.1016/0022-1694(78)90131-2.

Gash, J. H. C., Lloyd, C. R. & Lachaud, G. 1995 Estimating sparse forest rainfall interception with an analytical model. *Journal of Hydrology* **170** (1), 79–86. doi:10.1016/0022-1694(95)02697-N.

Ghimire, C. P., Bruijnzeel, L. A., Lubczynski, M. W. & Bonell, M. 2012 Rainfall interception by natural and planted forests in the Middle Mountains of Central Nepal. *Journal of Hydrology* **475**, 270–280. doi:10.1016/j.jhydrol.2012.09.051.

Ghimire, C. P., Bruijnzeel, L. A., Lubczynski, M. W., Ravelona, M., Zwartendijk, B. W. & van Meerveld, H. J. I. 2017 Measurement and modeling of rainfall interception by two differently aged secondary forests in upland eastern Madagascar. *Journal of Hydrology* **545**, 212–225. doi:10.1016/j.jhydrol.2016.10.032.

Ginebra-Solanellas, R. M., Holder, C. D., Lauderbaugh, L. K. & Webb, R. 2020 The influence of changes in leaf inclination angle and leaf traits during the rainfall interception process. *Agricultural and Forest Meteorology* **285–286**, 107924. doi:10.1016/j.agrformet.2020.107924.

Hassan, S. M. T., Ghimire, C. P. & Lubczynski, M. W. 2017 Remote sensing upscaling of interception loss from isolated oaks: Sardon catchment case study, Spain. *Journal of Hydrology* **555**, 489–505. doi:10.1016/j.jhydrol.2017.08.016.

Ji, Y. & Cai, T. J. 2015 Canopy interception in original Korean pine forest: measurement and dividual simulation in Xiaoxing'an Mountains, northeastern China. *Journal of Beijing Forestry University* **37** (10), 41–49. doi:10.13332/j.1000-1522.20150084.

Junqueira Junior, J. A., de Mello, C. R., de Mello, J. M., Scolforo, H. F., Beskow, S. & McCarter, J. 2019 Rainfall partitioning measurement and rainfall interception modelling in a tropical semi-deciduous Atlantic forest remnant. *Agricultural and Forest Meteorology* **275**, 170–183. doi:10.1016/j.agrformet.2019.05.016.

Klaassen, W., Bosveld, F. & Water, E. D. 1998 Water storage and evaporation as constituents of rainfall interception. *Journal of Hydrology* **212** (1–4), 36–50. doi:10.1016/S0022-1694(98)00200-5.

Leyton, L., Reynolds, E. R. C. & Thompson, F. B. 1967 Rainfall interception in forest and moorland. In: *International Symposium on Forest Hydrology* (W. E. Sopper & H. W. Lull, eds.). Pergamon, Oxford, pp. 163–178.

Liang, W. 2014 Simulation of Gash model to rainfall interception of *Pinus tabulaeformis*. *Forest Systems* **23** (2), 300–303. doi:10.5424/fs/2014232-03410.

Licata, J. A., Pypker, T. G., Weigandt, M., Unsworth, M. H., Gyenge, J. E., Fernández, M. E., Schlichter, T. M. & Bond, B. J. 2011 Decreased rainfall interception balances increased transpiration in exotic ponderosa pine plantations compared with native cypress stands in Patagonia, Argentina. *Ecohydrology* **4** (1), 83–93. doi:10.1002/eco.125.

Limousin, J., Rambal, S., Ourcival, J. & Joffre, R. 2008 Modelling rainfall interception in a mediterranean *Quercus ilex* ecosystem: lesson from a throughfall exclusion experiment. *Journal of Hydrology* **357** (1–2), 57–66. doi:10.1016/j.jhydrol.2008.05.001.

Linhoss, A. C. & Siegert, C. M. 2016 A comparison of five forest interception models using global sensitivity and uncertainty analysis. *Journal of Hydrology* **538**, 109–116. doi:10.1016/j.jhydrol.2016.04.011.

Liu, S. 1998 Estimation of rainfall storage capacity in the canopies of cypress wetlands and slash pine uplands in North-Central Florida. *Journal of Hydrology* **207** (1), 32–41. doi:10.1016/S0022-1694(98)00115-2.

Liu, Z., Wang, Y., Tian, A., Liu, Y., Webb, A. A., Wang, Y., Zuo, H., Yu, P., Xiong, W. & Xu, L. 2018 Characteristics of canopy interception and its simulation with a revised Gash model for a larch plantation in the Liupan Mountains, China. *Journal of Forestry Research* **29** (1), 187–198. doi:10.1007/s11676-017-0407-6.

Llorens, P. & Domingo, F. 2007 Rainfall partitioning by vegetation under Mediterranean conditions. A review of studies in Europe. *Journal of Hydrology* **335** (1–2), 37–54. doi:10.1016/j.jhydrol.2006.10.032.

Llorens, P. & Gallart, F. 2000 A simplified method for forest water storage capacity measurement. *Journal of Hydrology* **240** (1–2), 131–144. doi:10.1016/s0022-1694(00)00339-5.

Loustau, D., Berbigier, P., Granier, A. & Moussa, F. E. H. 1992 Interception loss, throughfall and stemflow in a maritime pine stand. I. Variability of throughfall and stemflow beneath the pine canopy. *Journal of Hydrology* **138** (3–4), 449–467. doi:10.1016/0022-1694(92)90130-n.

Ma, J., Zha, T., Jia, X., Tian, Y., Bourque, C. P. A., Liu, P., Bai, Y., Wu, Y., Ren, C., Yu, H., Zhang, F., Zhou, C. & Chen, W. 2018 Energy and water vapor exchange over a young plantation in northern China. *Agricultural and Forest Meteorology* **263**, 334–345. doi:10.1016/j.agrformet.2018.09.004.

Ma, C., Li, X., Luo, Y., Shao, M. & Jia, X. 2019 The modelling of rainfall interception in growing and dormant seasons for a pine plantation and a black locust plantation in semi-arid Northwest China. *Journal of Hydrology* **577**, 123849. doi:10.1016/j.jhydrol.2019.06.021.

Ma, C., Luo, Y. & Shao, M. 2020 Comparative modeling of the effect of thinning on canopy interception loss in a semiarid black locust (*Robinia pseudoacacia*) plantation in Northwest China. *Journal of Hydrology* **590**, 125234. doi:10.1016/j.jhydrol.2020.125234.

National Forestry and Grassland Administration 2013 China Forestry Statistical Yearbook. Available from: http://www.forestry.gov.cn/data.html/ (accessed 7 April 2019).

Owens, M. K., Lyons, R. K. & Alejandro, C. L. 2006 Rainfall partitioning within semiarid juniper communities: effects of event size and canopy cover. *Hydrological Processes* **20** (15), 3179–3189. doi:10.1002/hyp.6326.

Sadeghi, S. M. M., Attarod, P., Van Stan, J. T., Pypker, T. G. & Dunkerley, D. 2015 Efficiency of the reformulated Gash's interception model in semiarid afforestations. *Agricultural and Forest Meteorology* **201**, 76–85. doi:10.1016/j.agrformet.2014.10.006.

Sheng, H. C., Cai, T. J., Li, Y. & Liu, Y. J. 2014 Rainfall redistribution in *Larix gmelinii* forest on northern of Daxing'an mountains, north-east of China. *Journal of Soil and Water Conservation* **28** (06), 101–105. doi:10.13870/j.cnki.stbcxb.2014.06.019.

Shinohara, Y., Levia, D. F., Komatsu, H., Nogata, M. & Otsuki, K. 2015 Comparative modeling of the effects of intensive thinning on canopy interception loss in a Japanese cedar (*Cryptomeria japonica* D. Don) forest of western Japan. *Agricultural and Forest Meteorology* **214–215**, 148–156. doi:10.1016/j.agrformet.2015.08.257.

Su, L., Zhao, C., Xu, W. & Xie, Z. 2016 Modelling interception loss using the revised Gash model: a case study in a mixed evergreen and deciduous broadleaved forest in China. *Ecohydrology* **9** (8), 1580–1589. doi:10.1002/eco.1749.

Sun, J., Gao, P., Li, C., Wang, R., Niu, X. & Wang, B. 2019 Ecological stoichiometry characteristics of the leaf–litter–soil continuum of *Quercus acutissima* Carr. and *Pinus densiflora* Sieb. in Northern China. *Environmental Earth Sciences* **78** (1). doi:10.1007/s12665-018-8012-3.

Teklehaimanot, Z., Jarvis, P. G. & Ledger, D. C. 1991 Rainfall interception and boundary layer conductance in relation to tree spacing. *Journal of Hydrology* **123** (3–4), 261–278. doi:10.1016/0022-1694(91)90094-x.

Valente, F., David, J. S. & Gash, J. H. C. 1997 Modelling interception loss for two sparse eucalypt and pine forests in central Portugal using reformulated Rutter and Gash analytical models. *Journal of Hydrology* **190** (1), 141–162. doi:10.1016/S0022-1694(96)03066-1.

Valente, F., Gash, J. H., Nóbrega, C., David, J. S. & Pereira, F. L. 2020 Modelling rainfall interception by an olive-grove/pasture system with a sparse tree canopy. *Journal of Hydrology* **581**, 124417. doi:10.1016/j.jhydrol.2019.124417.

van Dijk, A. I. J. M. & Bruijnzeel, L. A. 2001a Modelling rainfall interception by vegetation of variable density using an adapted analytical model. Part 1. Model description. *Journal of Hydrology* **247** (3), 230–238. doi:10.1016/S0022-1694(01)00392-4.

van Dijk, A. I. J. M. & Bruijnzeel, L. A. 2001b Modelling rainfall interception by vegetation of variable density using an adapted analytical model. Part 2. Model validation for a tropical upland mixed cropping system. *Journal of Hydrology* **247** (3), 239–262. doi:10.1016/S0022-1694(01)00393-6.

Wallace, J. & McJannet, D. 2008 Modelling interception in coastal and montane rainforests in northern Queensland, Australia. *Journal of Hydrology* **348** (3–4), 480–495. doi:10.1016/j.jhydrol.2007.10.019.

Wei, X., Liu, S., Zhou, G. & Wang, C. 2005 Hydrological processes in major types of Chinese forest. *Hydrological Processes* **19** (1), 63–75. doi:10.1002/hyp.5777.

Zeng, N., Shuttleworth, J. W. & Gash, J. H. C. 2000 Influence of temporal variability of rainfall on interception loss. Part I. Point analysis. *Journal of Hydrology* **228** (3), 228–241. doi:10.1016/S0022-1694(00)00140-2.

Zhang, S., Li, X., Jiang, Z., Li, D. & Lin, H. 2018 Modelling of rainfall partitioning by a deciduous shrub using a variable parameters Gash model. *Ecohydrology* **11** (7), e2011. doi:10.1002/eco.2011.

First received 15 December 2019; accepted in revised form 18 August 2020. Available online 14 September 2020